Heliyon 10 (2024) e39890

Contents lists available at ScienceDirect

Heliyon

journal homepage: www.cell.com/heliyon

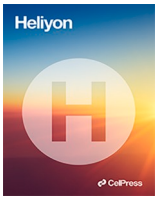

Research article

Lactucin ameliorates FFA-induced steatosis in HepG2 cells by modulating mitochondrial homeostasis through the SIRT1/PGC-1α signaling axis

Yi Lei [a,1], Xiao-li Ma [a,b,1], Tong Liu [d], Meng-jiao Wang [a], Jin-sen Kang [a,b], Jian Yang [a,b,*], Na Mi [b,c,**]

[a] College of Pharmacy, Xinjiang Medical University, Urumqi, 830011, China
[b] Key Laboratory of Active Components of Xinjiang Natural Medicine and Drug Release Technology, Urumqi, 830000, China
[c] Clinical Medicine Research Institute, the First Affiliated Hospital of Xinjiang Medical University, Urumqi, 830054, China
[d] Basic Medical College, Xinjiang Medical University, Urumqi, 830011, China

ARTICLE INFO

Keywords:
Lactucin
Mitochondrial biosynthesis
Mitochondrial dynamics
HepG2 cells

ABSTRACT

Nonalcoholic fatty liver disease is a complex disease involving abnormal liver metabolism. Its strong association with metabolic dysfunction has led to a change in nomenclature to metabolism dysfunction-associated fatty liver disease (MAFLD). MAFLD pathogenesis involves abnormal accumulation of hepatic lipids that lead to the production of excess free fatty acids (FFAs), which in turn cause an imbalance in hepatic mitochondrial function. Lactucin, a natural compound extracted from *Cichorium glandulosum* Boiss. et Huet, regulates liver metabolism and protects the liver. However, the potential mechanisms underlying the lactucin-mediated effects in MAFLD require further investigation. In the present study, HepG2 cells were treated with FFAs to establish an *in vitro* model of MAFLD. Parameters related to lipid accumulation and mitochondrial function, including triglycerides (TG), oil red O-stained lipid droplets, reactive oxygen species (ROS), mitochondrial membrane potential (JC-1), adenine triphosphate (ATP), and complex III were analysed. Morphology of the mitochondria were evaluated by transmission electron microscopy. Furthermore, key proteins in the sirtuin 1 (SIRT1)/peroxisome proliferator-activated receptor gamma coactivator-1α (PGC-1α) signalling axis and mitochondrial quality control were analysed. The SIRT1 inhibitor EX-527 was used to verify the key role of the SIRT1 signalling pathway. Western blotting showed that lactucin upregulated the expression of SIRT-1, PGC-1α, Nrf1, Tfam, Mfn2, and Opa1, and promoted mitochondrial biosynthesis and kinetics. The results suggest that lactucin restores mitochondrial dynamic homeostasis by upregulating the SIRT1/PGC-1α signalling axis, thereby reducing FFA-induced lipid accumulation in HepG2 cells.

* Corresponding author. School of Pharmacy, Xinjiang Medical University, No. 393, Beijing Road, Xinshi District, Urumqi 830017, Xinjiang Uygur Autonomous, China.
** Corresponding author. Clinical Medicine Research Institute, the First Affiliated Hospital of Xinjiang Medical University, No. 393, Beijing Road, Xinshi District, Urumqi, 830054, Xinjiang Uygur Autonomous, China.
E-mail addresses: yj365@hotmail.com (J. Yang), mina2a@163.com (N. Mi).
[1] Yi Lei and Xiao-li Ma contributed equally to this work.

https://doi.org/10.1016/j.heliyon.2024.e39890
Received 8 May 2024; Received in revised form 25 October 2024; Accepted 25 October 2024
Available online 26 October 2024

1. Introduction

Nonalcoholic fatty liver disease is a complex disease, and because of its strong association with abnormal liver metabolism it has been redefined as metabolism dysfunction-associated fatty liver disease (MAFLD). Patients with obesity, type 2 diabetes or hyperlipidemia have an increased risk of developing MAFLD [1]. Epidemiological studies have shown that MAFLD affects approximately 30 % of the global population [2]. Therefore, it represents one of the most common public health concerns. No effective treatments or specific drugs are available for the clinical management of MAFLD [3]. According to the classical "two-hit theory" [4] of MAFLD pathogenesis, abnormal accumulation of hepatic lipids leads to the production of excessive free fatty acids (FFAs), which in turn promote the oxidation of fatty acids in the liver and production of excessive superoxides, which impair hepatic mitochondrial functions and aggravate hepatic lipid metabolic abnormalities [5]. Existing studies indicate that mitochondrial dysfunction is a crucial factor in MAFLD pathogenesis and plays an important role in the pathological progression of steatosis [6]. Therefore, the present study focused on drugs that ameliorate hepatic mitochondrial damage and inhibit hepatic lipid accumulation to treat MAFLD.

Lactucin, a sesquiterpene lactone extracted from the edible medicinal plant *Cichorium glandulosum* Boiss et Huet (*C. glandulosum*), regulates liver metabolism, protects the liver, and exerts anticancer effects. *C. glandulosum* is an annual herbaceous plant of the genus Chicory in the family Asteraceae that has hepatoprotective, hypoglycaemic, and digestive properties [7]. In a previous study, we found that whole herbal extract of Chicory effectively attenuated lipid accumulation in the liver tissues of db/db mice and improved the antioxidant capacity of the organism, which in turn attenuated liver injury [8]. The hepatoprotective activity of *C. glandulosum* has been extensively studied by various research groups, and its hepatoprotective and anti-hepatotoxic effects have been elucidated previously. Sesquiterpene lactone, a key compound in *C. glandulosum,* has been demonstrated to have hepatoprotective effects [9]. In mice, lactucin inhibits lipid deposition and improves fatty liver and glucose homeostasis *in vivo*. At the cellular level, lactucin affects lipid differentiation in 3T3-L1 cells by inhibiting JAK2/STAT3-mediated mitotic clonal expansion (MCE), and promotes cellular lipolysis through the IL-6/GP130-related signalling pathway [10]. A previous study confirmed the hypolipidemic effect of lactucin *in vitro* using an FFA-induced HepG2 steatosis cell model and examined its potential mechanism of action [11]. However, whether the lactucin-mediated effects in preventing and treating MAFLD are related to attenuation of hepatic mitochondrial damage remains unclear.

Hepatic mitochondrial dysfunction is a non-negligible etiological factor in the development of the first and second stages of MAFLD, and is characterised by reduced energy production and impaired redox balance [12]. Studies have reported that mitochondrial dysfunction mediated by oxidative stress and peroxisome proliferator-activated receptor gamma coactivator-1α (PGC-1α) is involved in the pathological changes in lipid metabolism via sirtuin 1 (SIRT1) in MAFLD [13]. SIRT1 is a target of many plant flavonoids that promote metabolic and anti-ageing effects [14]. Following activation by phytochemicals, SIRT1 regulates PGC-1α-mediated mitochondrial biogenesis and mitosis. Silencing of SIRT1 abrogates the promoting effect of blueberry juice and probiotics on PGC-1α expression, and the protective effect on mitochondrial dysfunction in MAFLD rats [15]. In addition, PGC-1α is a key regulatory factor for mitochondrial quality control in MAFLD [16,17]. Therefore, determining whether lactucin targets the SIRT1/PGC-1α signalling axis to protect cells from mitochondrial dysfunction, which has implications for the treatment of mitochondria-mediated MAFLD is crucial.

In this study, HepG2 cells were treated with FFA (oleic acid/palmitic acid [OA/PA] = 2:1) to establish an *in vitro* model of MAFLD. Using this model, we examined the mechanisms by which lactucin affects cellular lipid accumulation and mitochondrial dysfunction. Insights into the mechanisms through which lactucin regulates mitochondrial biosynthesis and dynamics by targeting the SIRT1/PGC-1α signalling axis, and ameliorates lipid accumulation in FFA-induced HepG2 cells would help to elucidate the anti-MAFLD effect of lactucin.

2. Materials and methods

2.1. Materials

Palmitic and oleic acids were purchased from Sigma (San Francisco, CA, USA). The CCK-8 reagent kit was purchased from Tongren Chemical Technology Co. (Dojindo, Japan). Oil Red O, reactive oxygen species (ROS), Hoechst 33342, and mitochondrial respiratory chain complex III kit were purchased from Solebao Technology Co. (Beijing, China). The triglyceride (TG) enzyme assay kit was purchased from Applygen Technologies Ltd. (Beijing, China). Adenosine triphosphate (ATP), JC-1, and cellular mitochondrial isolation kit. MitoTracker™ Red was purchased from Thermo Fisher Scientific (Massachusetts, USA). Sodium dodecyl sulfate polyacrylamide gel electrophoresis (SDS-PAGE) gel preparation kit was purchased from Beyotime Biotechnology (Shanghai, China). All PCR reagents were purchased from Takara Biomedical Technology Co. (Beijing, China). Lactucin (purity ≥98 %) was obtained from the Xinjiang Institute of Physical and Chemical Technology, Chinese Academy of Sciences.

2.2. Cell culture

The human hepatocellular carcinoma cell line HepG2 was cultured in high-glucose Dulbecco's modified Eagle's medium (DMEM; HyClone™, GE Healthcare Life Sciences, Logan, UT, USA) supplemented with 10 % fetal bovine serum (FBS; Biological Industries, Israel), 1 % penicillin-streptomycin solution (HyClone™, USA), and 1 % GlutaMAX™-1 (Gibco, USA) in a 5 % CO_2 incubator at 37 °C.

2.3. Cell viability assay

Pipette 150 μL of medium containing HepG2 cells (6×10^4 cells/mL) evenly spread in a 96-well culture plate and incubated for 12 h until they completely adhered to the plate. The cells were divided into control and lactucin groups (5, 10, 20, 40, 80, and 160 μM). The control group was treated with only complete medium for calibration. The treatment groups were treated with the appropriate concentration of lactucin, and the cells were incubated for 48 h. CCK-8 reagent (1/10th volume of the culture medium) was added to the cells, and the cells were further incubated for 1 h. The absorbance (optical density [OD]) was measured at 450 nm using a plate reader.

2.4. TG level analysis

TG content in the cells from the different experimental groups was determined using a high-ester-sample TG Enzyme Assay Kit. Cells growing in 6-well plates were divided into control (CT), model (induced with 0.4 mM FFA [OA:PA = 2:1]), and 5 μmol/L, 10 μmol/L, and 20 μmol/L lactucin groups. The cells were treated for 48 h.

After the intervention, 0.1 mL lysis solution was added to 1×10^6 cells and incubated at room temperature for 10 min. The cells were gently scraped using a cell scraper and transferred to a 1.5 mL Eppendorf tube (ET). The supernatant (80 μL) was transferred to a 1.5 mL centrifuge tube (the remaining lysis solution was subjected to protein quantification to normalise the TG content), heated at 70 °C for 10 min, and centrifuged at 2000 rpm at room temperature for 5 min. The TG content in the samples were determined by measuring the OD of each group at 550 nm.

2.5. Oil red O staining

Oil red O, a strong dye that easily combines with TGs to form lipid droplets, was used to stain the intracellular lipid droplets. HepG2 cells in growth phase were uniformly plated in 6-well plates containing 3–5 sterile circular (0.8 cm) coverslips per well and cultured for 12 h to allow the cells to adhere. Treat the control, FFA model, and different concentrations of lactucin groups for 48 h.

At the end of the treatment, the cell culture plate was removed from the incubator, the medium was discarded, and the cells were washed once with phosphate buffered saline (PBS), fix the fixative for 15 min, washed again with PBS, and the supernatant was discarded. Then, coverslips were immersed in 60 % isopropanol, and the solution was discarded. Oil red O staining solution (50 μL) was dripped onto each coverslip in the dark for 20 min. The dye solution was then discarded, and the cells were washed with distilled water to remove any residual stain. Mayer's hematoxylin staining solution was added dropwise to each coverslip, and the nuclei were stained for 140 s. The staining solution was then aspirated, and the coverslips with cells were washed thrice with distilled water. The cell side of the coverslip was mounted horizontally onto a slide with an anti-fluorescence quenching sealer and shielded from light for 2 h. Finally, the cells were viewed under an inverted microscope, and images were captured.

2.6. Quantification of intracellular ATP

Firefly luciferase oxidises luciferin in an ATP-dependent manner, and the fluorescence generated (within a certain concentration range) is proportional to the concentration of ATP. An ATP detection kit was used to evaluate changes in ATP levels in HepG2 cells. The cells were treated according to the manufacturer's instructions and relative light units (RLUs) were determined using a multifunctional enzyme marker. The ATP concentration of the sample was calculated based on the standard curve, and the protein concentration was determined using a BCA assay kit. ATP was quantified as RLUs and converted into nmol ATP/mg protein based on the calibration curve.

2.7. Determination of ROS

ROS detection was based on the fluorescent probe DCFH-DA. ROS oxidises non-fluorescent DCFH to fluorescent DCF via a series of reactions inside the cell; the level of intracellular ROS is proportional to the fluorescence intensity of DCF. HepG2 cells were inoculated in 35 mm laser confocal glass bottom dishes and treated with the blank control, FFA, Rosup (ROS positive control reagent; 50 mg/mL, diluted 1:1000), or 20 μM lactucin for 48 h. The medium was then discarded, the cells were washed once with PBS, an appropriate amount of diluted positive control solution was added to the positive control group, and the plates were incubated at 37 °C for 20 min. DCFH-DA (10 μmol/L) was added to each well, and the plates were incubated for 20 min at 37 °C. The cells were washed thrice with serum-free culture medium, visualised by laser confocal microscopy, and images were captured.

2.8. Mitochondrial membrane potential ($\Delta\Psi m$)

The JC-1 fluorescent probe exhibits potential-dependent aggregation states that produce different fluorescence signals in the mitochondrial matrix within the cell. The degree of mitochondrial depolarisation is measured based on the relative proportion of different fluorescence signals. Carbonyl cyanide 3-chlorophenylhydrazone (CCCP) was used as a positive control for changes in the intracellular mitochondrial membrane potential. Following treatment, HepG2 cells were incubated at 37 °C for 48 h, and an appropriate amount of JC-1 stain (working solution) was added to the cells and mixed thoroughly. The cells were incubated in a 37 °C incubator for 20 min, and then washed twice with JC-1 staining buffer (1 ×). An appropriate amount of cell culture medium was added

and the cells were observed by laser confocal microscopy and images were captured.

2.9. Complex III

Mitochondrial complex III is an important component of the energy conversion process and is widely found in the mitochondria of animals and plant cells.

(1) Isolation of mitochondria: Disrupted cells were collected in EP tubes. Mitochondrial isolation reagent (1 mL, phenylmethylsulfonylchloride [PMSF]) was added to the cells and the cells were resuspended and incubated on ice for 20 min. The cell suspension was then aspirated into a 5 mL homogeniser and homogenised with approximately 20 strokes. The homogenate was transferred to a fresh EP tube and centrifuged at a low temperature at 600×*g* for 10 min. The supernatant was aspirated into a new centrifuge tube and centrifuged at 11,000×*g* at low temperature for 10 min. The pellet contained the mitochondria-enriched fraction.
(2) Extraction of mitochondrial proteins: Mitochondrial buffer (200 μL of PMSF) was added to the mitochondrial sample and the mitochondria were lysed on ice for 20 min followed by centrifugation at 13,523×*g* at 4 °C for 10 min. The supernatant was collected and stored on ice until further analysis.
(3) Determination of respiratory chain complex III: A coenzyme Q (CoQ)-cytochrome C reductase Activity Assay Kit was used to detect mitochondrial activity. The mitochondrial complex III was quantified by measuring the change in absorbance at 550 nm.

2.10. MitoTracker™ red

MitoTracker™ Red was used to stain mitochondria in living cells. The accumulation of the dye is dependent on the mitochondrial membrane potential. HepG2 cells were plated in 35 mm laser confocal glass bottom dishes and treated with the control, FFA, or 20 μM lactucin for 48 h. The medium was discarded, the cells were washed twice with PBS, and 1 mL of MitoTracker™ Red dye solution was added to each well in the ratio of MitoTracker™ Red: Hoechst 3334: complete medium (1:10:1000). The cells were incubated for 25 min at 37 °C in a cell culture incubator. Then, the cells were washed twice with PBS, an appropriate amount of culture medium was added to the wells, and laser confocal images were obtained.

2.11. Transmission electron microscopy (TEM)

The cells in the CT, FFA, and 20 μM lactucin groups were treated with the corresponding drug for 48 h. Half of the original volume of complete culture medium was then aspirated and an equal volume of preheated (37 °C) 2.5 % glutaraldehyde (EM grade) fixative was added. The mixture was shaken gently for homogeneous distribution of the fixative, and the cells were fixed for 10 min in a 37 °C incubator. The fixative was discarded, 2 mL of 2.5 % glutaraldehyde EM fixative was quickly added to each dish, and the cells were fixed for 2 h in the dark. The fixative was aspirated, PBS was added, and the samples were stored in a refrigerator at 4 °C until embedding and further processing. Mitochondrial morphology was observed using TEM.

2.12. Quantitative real-time PCR analysis (qRT-PCR)

The effects of lactucin on the mRNA expression of *SIRT1*, key regulators of mitochondrial biosynthesis (*PGC-1α*, *Nrf1*, and *Tfam*), and mitochondrial kinetics genes (*Mfn2*, *Opa1*, and *Drp1*) were examined by qRT-PCR. The primers were designed and synthesised by Sangon Biotech Co., Ltd., and are listed in Table 1.

HepG2 cells were inoculated in 6-well plates corresponding to the control, FFA, and FFA +20 μmol/L lactucin groups, and the interventions were carried out for 48 h. RNA was extracted using TRIzol® and chloroform ($CHCl_3$), and RNA purity and concentration were determined using a NanoDrop™ 2000 ultramicro spectrophotometer. Reverse transcription and qRT-PCR were performed according to the manufacturer's instructions. The difference between the average C_t value of the target gene and that of the internal reference represented Δt, and the relative expression of the target gene was calculated as $2^{(-\Delta\Delta Ct)}$.

Table 1
Primers for qRT-PCR.

Gene	Species	5′-Forward primer sequence-3′	5′-Reverse primer sequence-3′
SIRT1	Human	ACTTCAGGTCAAGGGATGGT	TTCCACTGCACAGGCACATAC
PGC-1α	Human	GATGAAGGGTACTTTTCTGCCCCT	TGAGGAGGGTCATCGTTTGTG
Nrf1	Human	TGCCGTGGCTGATGGAGAGG	GATGCTTGCGTCGTCTGGATGG
Tfam	Human	GCGTTGGAGGGAACTTCCTGATTC	ATACCTGCCACTCCGCCCTATAAG
Mfn2	Human	GCAATGTCCCTGCTCTTCTCTC	TCTTGGCACTCCTCTTTTCCTCT
Opa1	Human	ACCGTTAGCCCTGAGACCATATCC	GCGTTCAGCATCCACAGATCCATC
Drp1	Human	ATCCAGCTGCCTCAAATCGT	AGCTGGCTCCTTATTTTTGGTGT
SREBP1	Human	TTCCGAGGAACTTTTCGCCG	CCTCGTACGGCCCTTCCTA
GAPDH	Human	CAGGAGGCATTGCTGATGAT	GAAGGCTGGGGCTCATTT

2.13. Western blotting

SIRT1, PGC-1α, Nrf1, Tfam, Mfn2, Opa1, and Drp1 protein levels were detected by western blotting (Antibody information is shown in Table 2). Pretreated cells suspended in cell lysis buffer (containing PMSF protease inhibitor) was mixed with 5 × loading (4:1) and the samples were boiled at 100 °C for 15 min. An SDS-PAGE gel preparation kit was used to prepare an 8–12 % gel based on the molecular weight of the target protein. Protein samples were loaded in in the gel and separated by electrophoresis. Proteins in the gel were electrotransferred onto a Nitro-Cellulose membrane (NC) membrane. The NC membrane was blocked with 5 % milk for 1 h, followed by incubation with the corresponding primary and secondary antibodies for 1–2 h. Enhanced chemiluminescence (ECL) solution was added dropwise for colour development. The ImageJ image analysis software was used for grey value analysis. Glyceraldehyde 3-phosphate dehydrogenase (GAPDH) was used as an internal reference to calculate the relative expression of the target protein in each group.

2.14. Statistical analyses

GraphPad Prism 9.5 software was used for statistical analysis. All experiments were repeated at least three times independently, and significant differences between groups were assessed using one-way analysis of variance (ANOVA). A *post hoc* test was performed using Tukey's multiple comparisons test. The data are expressed as the mean ± standard deviation (SD). Statistical significance was set at $P < 0.05$.

3. Results

3.1. Effect of lactucin on cell viability

The CCK-8 assay was used to evaluate the potential toxicity of lactucin in HepG2 cells. The results showed no significant cytotoxicity of lactucin in the concentration range of 0–20 μM. Significant cytotoxicity was observed at a concentration of 40 μM, and the cytotoxicity increased in a concentration-dependent manner as lactucin concentration increased to 80–160 μM. The IC_{50} value of lactucin was determined to be 271.8 μmol/L. Morphological assessment of HepG2 cells using an inverted microscope following treatment with 0, 5, 10, or 20 μM lactucin for 48 h revealed good growth status, normal morphology, strong adhesion and growth abilities of the cells with no significant difference between the groups (Fig. 1A–C). Therefore, 5, 10, and 20 μM lactucin were used for drug treatment in the subsequent experiments.

3.2. Intracellular lipid accumulation

Oil red O staining revealed that FFA treatment promoted the accumulation of lipid droplets compared with that in the control group, whereas the formation of red lipid droplets was significantly reduced following treatment with 10 μM and 20 μM lactucin compared with that in the model group (Fig. 1F and G). To further verify the inhibitory effect of lactucin on FFA-induced lipid accumulation, TG accumulation was measured in HepG2 cells. As shown in Fig. 1D, the TG content was significantly higher in the FFA-treated model group than that in the control group, but this effect was significantly inhibited in a concentration-dependent manner in the lactucin-treated group. These results suggest that an FFA-induced *in vitro* fat accumulation model of HepG2 cells was successfully established. Lactucin-mediated inhibitory effect on fat accumulation was the most significant in the 20 μM group, which was further confirmed by qRT-PCR analysis of the relative mRNA expression of *SREBP-1* (Fig. 1E).

3.3. Effect of lactucin on FFA-induced changes in mitochondrial function in HepG2 cells

TEM revealed swollen mitochondria with permeable matrix, broken cristae, and fragmented bilayer membrane in FFA-treated cells in the model group compared with those in the control group. Lactucin treatment restored the integrity of the mitochondrial bilayer membrane and intramembrane cristae, as evidenced by intact cristae (Fig. 2A and B).

The ATP content was significantly reduced in the cells in the FFA-induced model group relative to that in the control group;

Table 2
Information of antibodies.

Antibody	Company/Cat	Dilution	Molecular weight (kDa)
SIRT1	Abcam/ab 189494	1:1000	110
PGC-1α	Cell Signaling Technology/2178S	1:1000	130
Nrf1	Abcam/ab 175932	1:2000	68
Tfam	Abcam/ab 176558	1:1000	24
Mfn2	Abcam/ab 124773	1:2000	80
Opa1	Abcam/ab 157457	1:500	85
Drp1	Abcam/ab 184247	1:1000	83
GAPDH	Affinity Biosciences/AF 7021	1:5000	35
Goat Anti-Rabbit Ig, Human	Southern Blotech/4010-05	1:5000	/

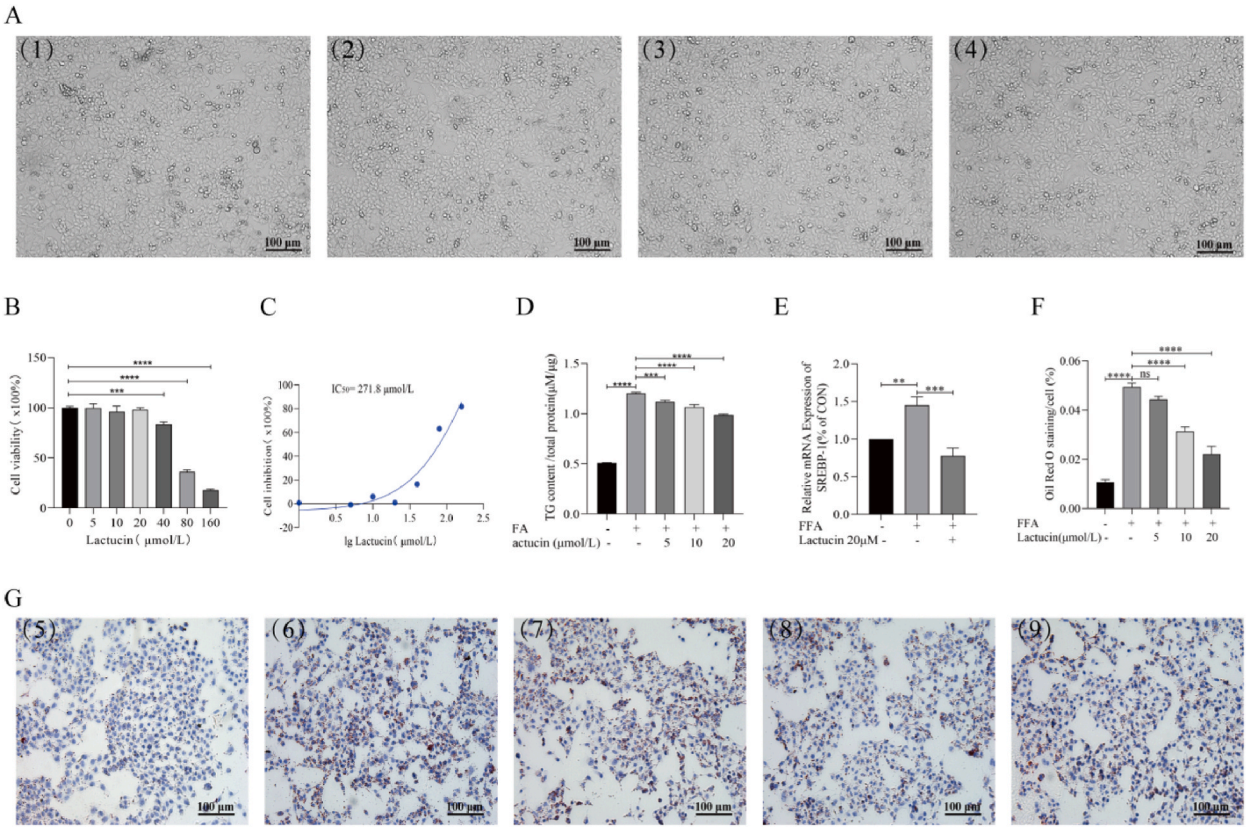

Fig. 1. Effects of lactucin on cell viability and intracellular lipid accumulation in HepG2 cells. (A) HepG2 cells were treated with 0 (1), 5 (2), 10 (3), or 20 (4) μmol/L lactucin for 48 h, and cell morphology was observed. (B) CCK-8 assay was used to measure the cell survival rate and IC50 (C). (D) The TG enzyme method was used to determine the changes in triglyceride content in HepG2 cells after FFA intervention and treatment with different concentrations of lactucin for 48 h. (E) RT–PCR was used to detect the mRNA levels of *SREBP-1* in cells. (F–G) Effect on intracellular lipid accumulation in HepG2 cells as observed by oil red O staining. (5) Control, (6) FFA (0.4 mM, OA:PA = 2:1), (7) FFA+5 μmol/L lactucin, (8) FFA+10 μmol/L lactucin, (9) FFA+20 μmol/L lactucin.

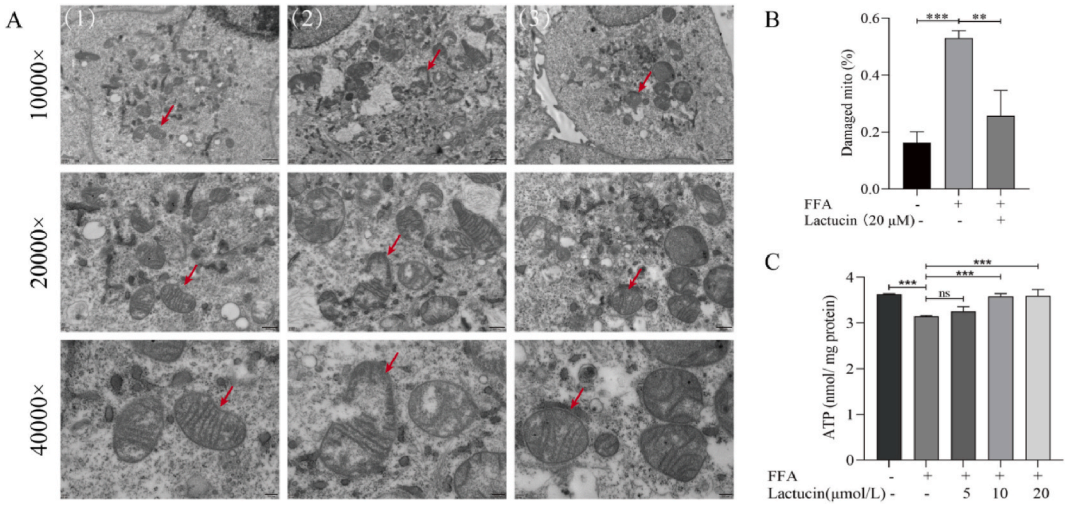

Fig. 2. Effect of lactucin on mitochondrial structure and ATP content in FFA-induced HepG2 cells. (A–B) Observation of mitochondrial ultrastructure by transmission electron microscopy. The red arrow indicates the same mitochondria at different magnifications. (1) Control, (2) FFA, and (3) FFA+20 μmol/L lactucin. (C) Intracellular ATP levels were measured using a kit.

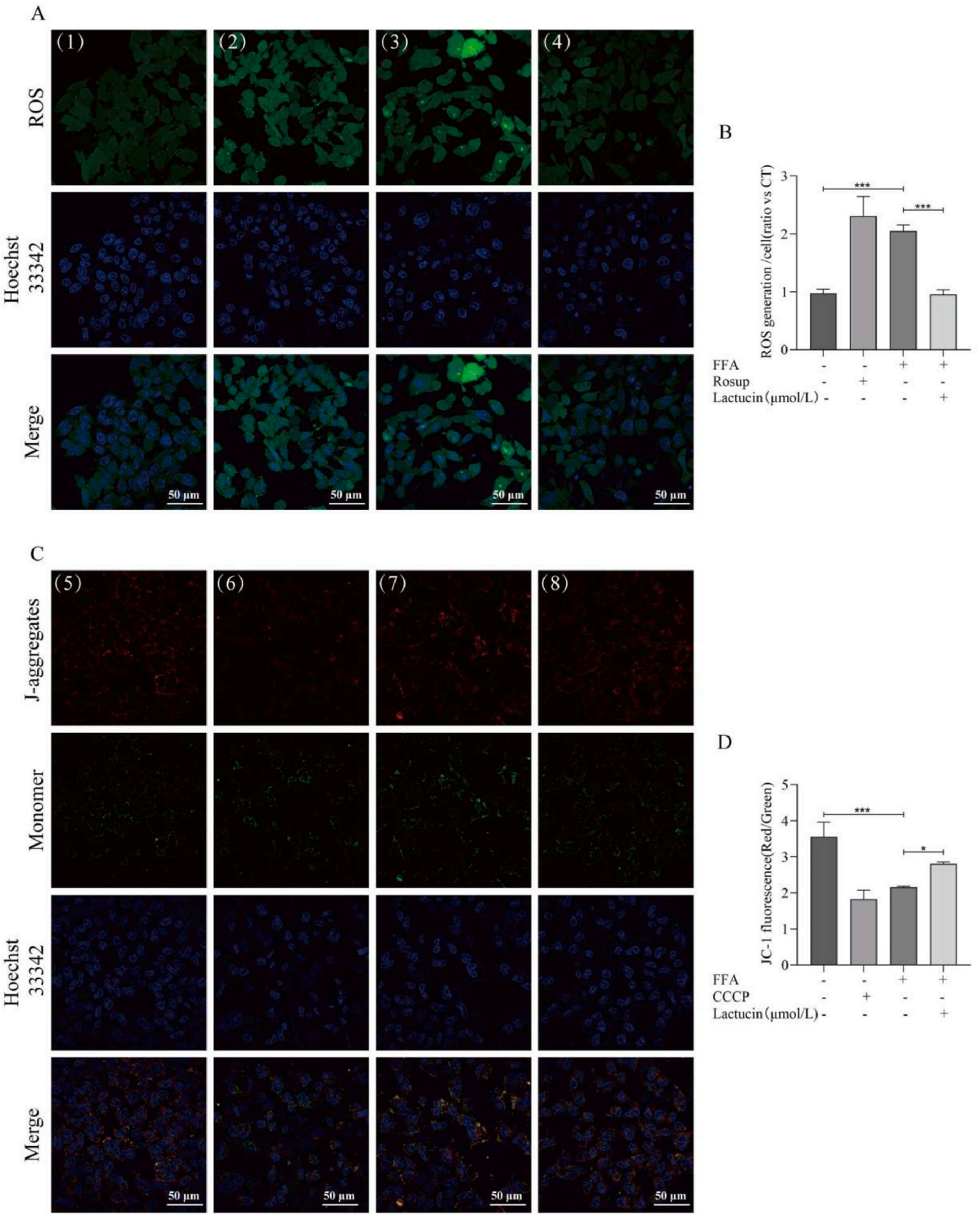

Fig. 3. Effects of Lactucin on FFA-induced changes in the mitochondrial membrane potential and ROS levels in HepG2 cells. (A) Detection of intracellular ROS levels using the fluorescent probe DCFH-DA. (1) Control, (2) Rosup, (3) FFA, and (4) FFA+20 μmol/L lactucin. (B) The relative fluorescence intensity corresponding to each group of ROS experiments. (C) Changes in the intracellular mitochondrial membrane potential. (5) Control, (6) CCCP, (7) FFA, and (8) FFA+20 μmol/L lactucin. (D) The relative fluorescence intensity corresponding to each group of JC-1-treated cells.

interestingly, the ATP content was not significantly different from that in the model group when lactucin treatment was administered at a concentration of 5 μM ($P > 0.05$), whereas it was significantly elevated at concentrations of 10 μM and 20 μM of lactucin compared to that in the model group, (Fig. 2C). Therefore, the 20 μM lactucin was selected for subsequent experiments.

The ROS level in the cells was measured by quantifying the fluorescence intensity of ROS in the cells using laser confocal scanning microscopy. As shown in Fig. 3A and B, ROS fluorescence intensity was highest in the Rosup-positive group. The fluorescence intensity in the FFA-induced model group was significantly higher than that of the control group, but this increase was significantly inhibited by lactucin.

The JC-1 assay for changes in mitochondrial membrane potential revealed weak red and strong green fluorescence in the CCCP-treated positive group, whereas the control group showed strong red and weak green fluorescence. Red fluorescence intensity in the FFA-induced model group was lower than that in the control group, whereas the green fluorescence intensity was higher. Interestingly, lactucin treatment significantly reversed this trend in the model group (Fig. 3C and D).

3.4. Effect of lactucin on the SIRT1/PGC-1α signalling axis and mitochondrial biosynthesis-related gene expression in FFA-induced HepG2 cells

Western blot analysis of key genes, including SIRT1, PGC-1α, Nrf1, and Tfam revealed that FFA treatment decreased SIRT1, PGC-1α, Nrf1, and Tfam expression levels in HepG2 cells. Compared with that in the model group, lactucin treatment significantly upregulated SIRT1, PGC-1α, Nrf1, and Tfam expression levels (Fig. 4E–L, refer to A-G in Multimedia component 1). Consistent with these results, RT-PCR analysis showed that the expression of *SIRT1*, *PGC-1α*, *Nrf1*, and *Tfam* was downregulated in the FFA-treated cells compared to that in the control cells, and this downregulation was significantly reversed by lactucin (Fig. 4A–D).

3.5. Effect of lactucin on the expression of genes related to mitochondrial dynamics in FFA-induced HepG2 cells

Western blot analysis of three key genes related to mitochondrial dynamics, including Mfn2, Opa1, and Drp1 revealed significantly lower expression levels of Mfn2 and OPA1 in FFA-treated HepG2 cells compared with that in the control group. Lactucin treatment significantly upregulated the expression of Mfn2 and Opa1 (Fig. 5B and C and 5E-F, refer to H-K in Multimedia component 1). Consistently, RT-PCR results showed that lactucin treatment significantly inhibited the downregulation of Mfn2 and OPA1 expression

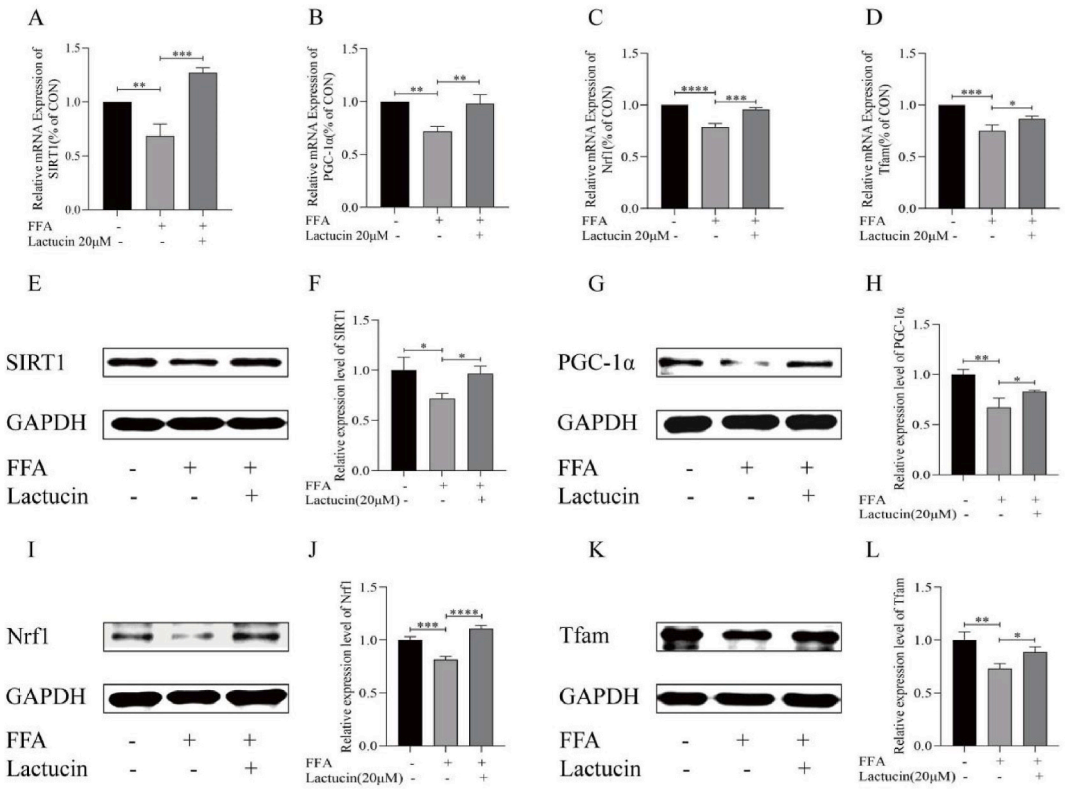

Fig. 4. Effect of lactucin on mitochondrial biosynthesis genes in FFA-induced HepG2 cells. (A–D) Expression of *SIRT1*, *PGC-1α*, *Nrf1*, and *Tfam* mRNA. (E–L) Protein expression of SIRT1, PGC-1α, Nrf1, and Tfam in different experimental groups and the relative intensity of each band for GAPDH quantification.

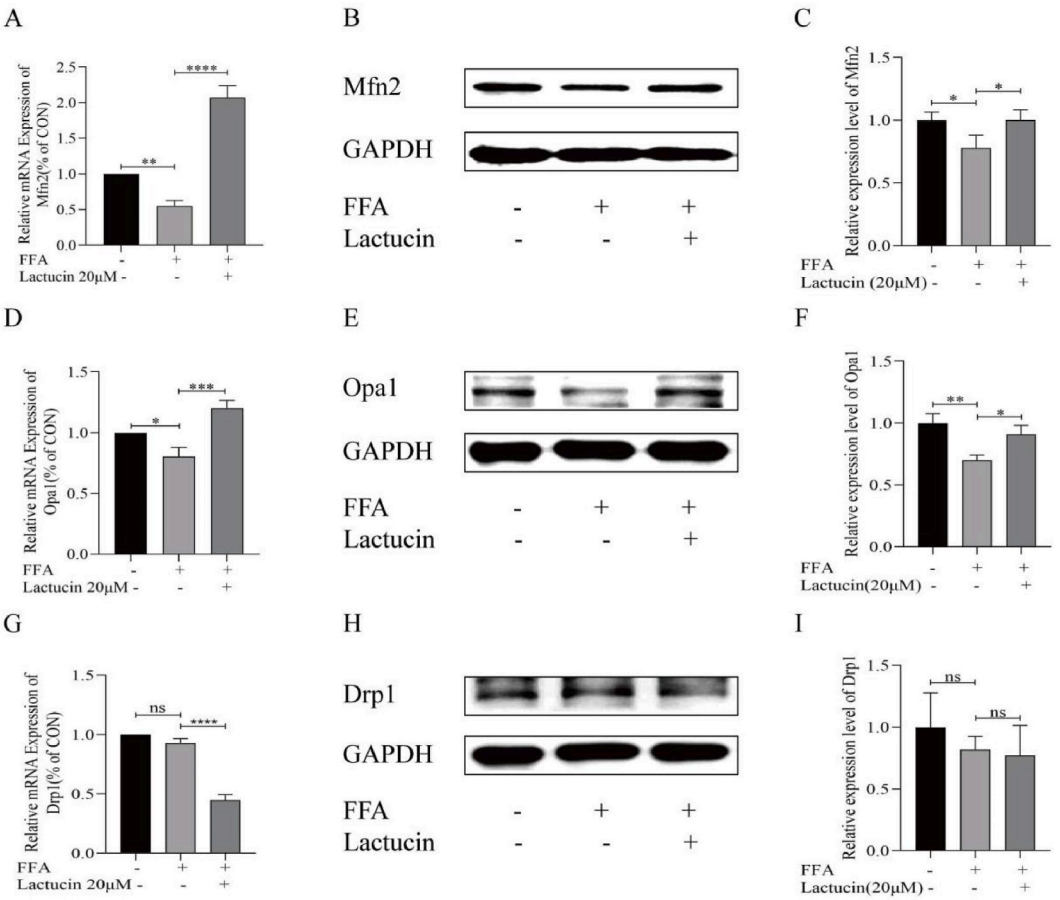

Fig. 5. Effect of lactucin on mitochondrial dynamics genes in FFA-induced HepG2 cells. (A–C) Expression of Mfn2 mRNA and protein. (D–F) Expression of Opa1 mRNA and protein. (G–I) Drp1 mRNA and protein expression.

in the FFA model group (Fig. 5A and D). However, RT-PCR results for the mitochondrial splitting factor Drp1 showed no significant difference between the FFA model and control groups ($P > 0.05$), whereas the lactucin-treated group showed significant down-regulation of Drp1 expression compared with that in the model group. At the protein level, there was no significant difference ($P > 0.05$) in Drp1 expression levels between the control, FFA model, and lactucin-treated groups (Fig. 5G–I, refer to L-M in Multimedia component 1).

3.6. *Effect of SIRT1 inhibition on lactucin-mediated amelioration of lipid accumulation and mitochondrial function*

As shown in Figure 6A-B, D the cell sheet in the FFA-induced model group appeared to have shrunk into thin strips, with a small proportion of cells displaying a round acellular morphology compared to the cells in the control group. Oil Red O staining followed by inverted microscopy revealed significantly increased formation of red lipid droplets in the FFA-induced model group. Interestingly, the cell morphology was partially restored, and the formation of red lipid droplets was significantly reduced following lactucin treatment. However, the lactucin-induced ameliorative effect was inhibited by treatment with EX527, a SIRT1 inhibitor. Consistently, EX527 inhibited the ability of lactucin to lower the intracellular TG level (Fig. 6G).

Analysis of mitochondrial membrane potential (ratio of red to green fluorescence intensity, Fig. 6C–E) revealed that lactucin treatment significantly increased the fluorescence intensity ratio of the FFA group, while the enhanced fluorescence intensity difference was weakened after EX527 treatment. Complex III activity in the cells showed the same trend (Fig. 6H). A MitoTracker™ Red fluorescent probe was used to observe the dispersion and activity of mitochondria in the cells. As shown in Fig. 6F, compared to the model group, mitochondria in the lactucin-treated group were evenly dispersed around the nucleus and exhibited strong fluorescence intensity. Following EX527 intervention, mitochondria clustered on one side of the nucleus and the fluorescence intensity was reduced.

3.7. *Effect of SIRT1 inhibition on mitochondrial quality control-related proteins*

As shown in Fig. 7A–L(refer to N-X in Multimedia component 1), the SIRT1 inhibitor EX527 regulated key proteins involved in

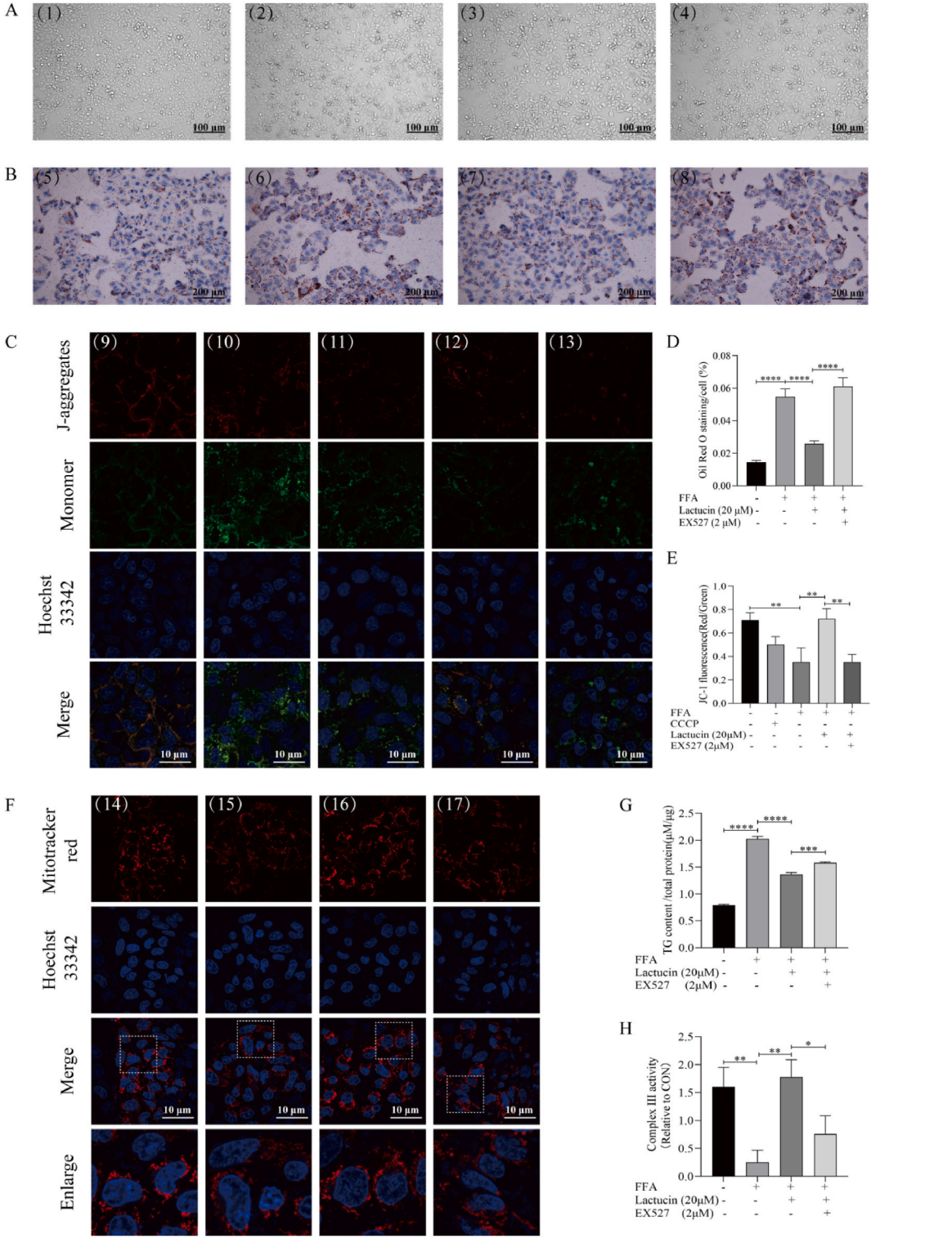

(caption on next page)

Fig. 6. The SIRT1 inhibitor EX527 reverses the effects of lactucin on lipid accumulation and mitochondrial function. (A) (1,5) Control, (2,6) FFA, (3,7) FFA+20 μmol/L lactucin, and (4,8) EX527 + FFA+20 μmol/L lactucin. HepG2 cells in different groups were treated for 48 h, and cell morphology was observed. (B, D) Oil red O staining was used to observe the changes in lipid accumulation in HepG2 cells of different groups. (C, E-F) Effects of EX527 on mitochondrial membrane potential and mitochondria, as observed under specific fluorescence. (9,14) Control, (10) CCCP (11,15) FFA (12,16) FFA+20 μmol/L lactucin, (13,17) EX527 + FFA+20 μmol/L lactucin. (G) Changes in triglyceride content in HepG2 cells after EX527 intervention as determined by TG enzyme assay. (H) Respiratory chain complex III activity was assayed using a CoQ-Cytochrome C reductase activity assay kit.

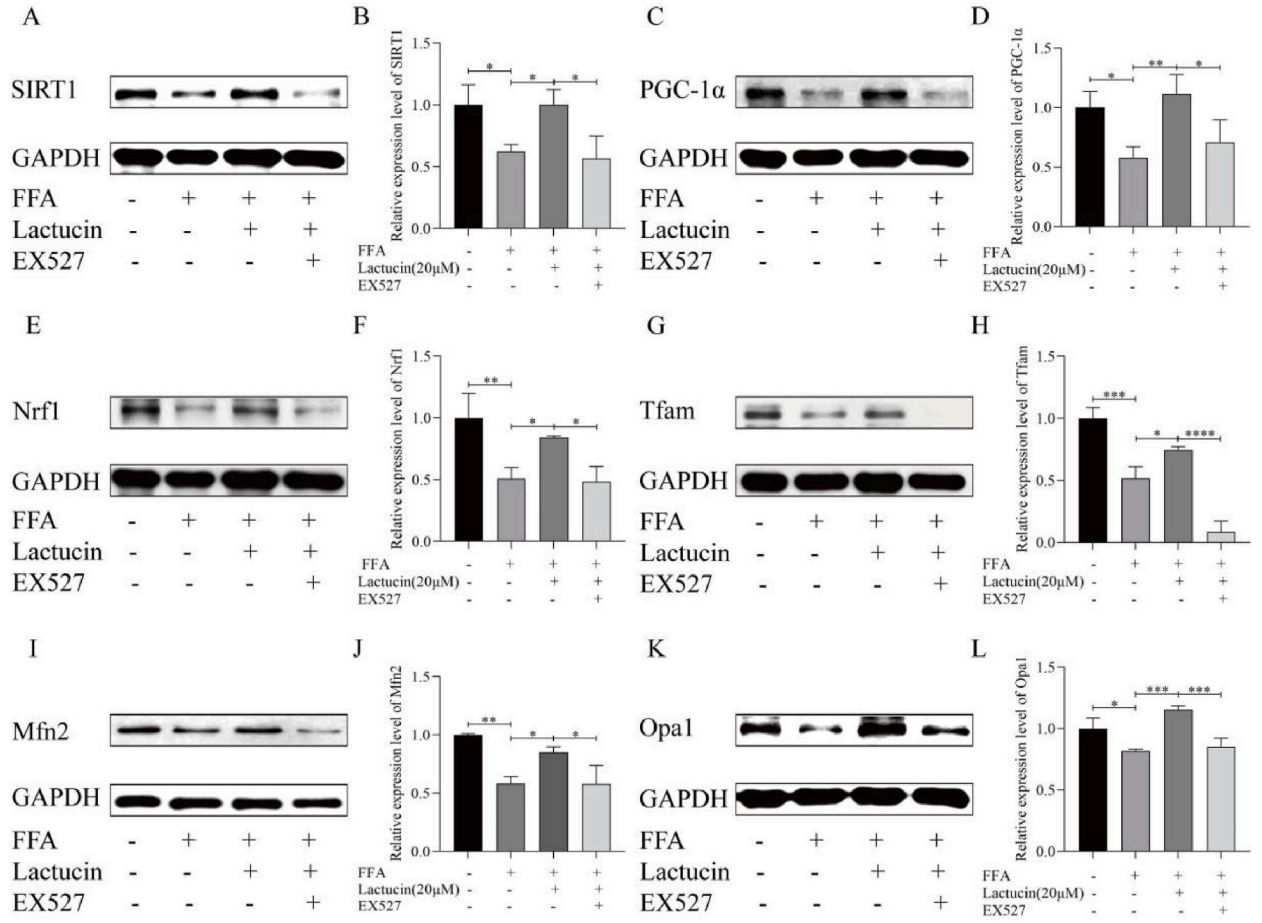

Fig. 7. The SIRT1 inhibitor EX527 reverses the effects of lactucin on mitochondrial quality control-associated proteins. (A–L) The effect of EX527 on intracellular SIRT1, PGC-1α, Nrf1, Tfam, Mfn2, and Opa1 protein levels was observed. The relative intensity of each protein band was quantified by GAPDH.

mitochondrial quality control. Compared with that in the FFA model group, the levels of SIRT1, PGC-1α, Nrf1, Tfam, Mfn2, and Opa1 were significantly higher in the lactucin-treated group. Moreover, EX527 treatment reversed the lactucin-induced increase in SIRT1, PGC-1α, Nrf1, Tfam, Mfn2, and Opa1 levels.

4. Discussion

The classical “two-hit theory” describes an important mechanism of MAFLD pathogenesis. Studies have shown that excessive FFAs promote fatty acid β-oxidation, damage the function of liver cell mitochondria, result in insufficient ATP production for normal liver cell functioning, leading to dysregulated lipid metabolism and impaired blood sugar and protein synthesis [5]. MAFLD is initially caused by excessive accumulation of fat in the liver, known as hepatic steatosis, with 5–20 % of patients with steatosis progressing to the more severe form of nonalcoholic steatohepatitis [18]. Without timely treatment and optimised diet, patients can develop irreversible liver fibrosis, cirrhosis, and cancer. Ethical issues and limited availability of human liver samples complicate the use of primary human cell cultures in studies [19]. Therefore, the HepG2 cell line provides a suitable alternative for such studies. HepG2, a hepatoblastoma cell line, is derived from human hepatocellular carcinoma tissue. The cells are highly differentiated, with complete

biotransformation of metabolic enzymes, and are homologous to normal human liver parenchymal cells. The metabolising enzymes remain stable for studies related to drug action and do not change with increased number of cell passages, rendering them suitable for use in study of hepatocyte metabolism [20]. Therefore, in the present study, HepG2 cells were used to generate an *in vitro* model of FFA-induced MAFLD to investigate the effects of lactucin on mitochondrial function, dynamics, and homeostasis.

4.1. Lactucin inhibits FFA-induced accumulation of lipid droplets in HepG2 cells

Excessive fat accumulation is an important feature of hepatocellular steatosis. FFAs constituted with different ratios of unsaturated fatty acids (OA) and saturated fatty acids (PA) were incubated with HepG2 cells to induce fat overload. FFA mixtures (OA/PA = 2:1) are used to generate cellular models of benign chronic steatosis [21]. Therefore, based on previous research [22], we treated HepG2 cells with 0.4 mM FFA (OA/PA = 2:1) to establish a MAFLD model (Fig. 1). Consistent with the results of previous studies, TG content in the FFA-treated group was significantly higher than that in the CT group. Oil Red O staining revealed the accumulation of lipid droplets in the cells under an inverted microscope. In addition, we detected a significant increase in the relative *SREBP1* mRNA expression in the FFA-treated group. SREBP1, located in the endoplasmic reticulum, acts as a transporter to regulate intracellular cholesterol level and participates in cholesterol homeostasis [23]. These results suggest that a high-fat model of FFA-induced HepG2 cells was successfully established. Moreover, TG content, relative *SREBP1* mRNA content, and red lipid droplet formation were effectively inhibited by lactucin treatment compared with those in the FFA model group. These results suggest that lactucin improves hepatic steatosis by reducing intracellular lipid droplets.

4.2. Lactucin improves mitochondrial function in lipid-accumulating cells

Mitochondria participate in a series of physiological processes including ATP production, free radical release, FFA oxidation, and cholesterol synthesis [24]. Further studies have confirmed that mitochondrial dysfunction is a key feature of MAFLD. The second strike in the MAFLD pathogenesis is characterised by chronic stress, including ROS production, exacerbation of pro-inflammatory responses, fatty liver-associated endoplasmic reticulum stress, augmentation of lipid peroxidation, and mitochondrial damage [25,26]. In MAFLD cell models, activation of SIRT1/NRF2 signal transduction and ROS scavenging inhibit oxidative stress, alleviate mitochondrial dysfunction, and inhibit lipid accumulation [27]. As shown in Figs. 2 and 3, the ATP content decreased, ROS consumption increased, and the mitochondrial membrane potential decreased in the FFA model group. In addition, TEM revealed disruption of mitochondrial ultrastructure with double-layer membrane rupture, matrix transparency, and crista rupture. Both mitochondrial morphology and related indicators suggest disruption of cellular mitochondrial function in the FFA model group. However, treatment with lactucin improved mitochondrial dysfunction, increased ATP content, and reduced ROS content, and effectively restored the mitochondrial membrane potential.

4.3. Effect of lactucin on genes related to mitochondrial biogenesis

SIRT1 is a member of the silent information regulator protein family and is dependent on nicotinamide adenine dinucleotide deacetylases. It is distributed in the nucleus and plays important roles in key physiological and pathological processes in the liver, such as lipid metabolism, fatty acid oxidation, inflammation, and mitochondrial dysfunction [28–30]. The regulation of cellular energy may also be related to SIRT1 enzyme activity. Studies have reported that SIRT1 activates the PGC-1α deacetylation pathway, which in turn activates mitochondrial function and fatty acid oxidation, thereby improving lipid metabolism disorders [31–33]. PGC-1α is a powerful transcriptional coregulator of mitochondrial genes, including those involved in the electron transport systems [34]. In the present study, lactucin treatment activated SIRT1 and downstream PGC-1α signalling, and upregulated the mRNA and protein levels of Nrf1 and Tfam. Together with the effects of lactucin on mitochondrial morphology and energetics, these findings suggest that lactucin may regulate mitochondrial biogenesis by activating the SIRT1/PGC-1α signalling axis, inhibiting lipid accumulation, and subsequently improving the damage caused by FFAs in HepG2 cells.

4.4. Effect of lactucin on genes related to mitochondrial dynamics

Mitochondrial dynamics involve processes, regulated by relevant proteins, through which mitochondria constantly undergo fusion and fission cycles to maintain their shape, distribution, and size. The mitochondrial splitting factor (DRP1), outer membrane fusion factor (Mfn2), and inner membrane fusion factor (Opa1) constitute key factors that regulate mitochondrial dynamics [35]. In a study on fatty liver haemorrhagic syndrome (FLHS) hens, the mRNA expression of Mfn2 and OPA1 was significantly reduced, whereas that of Drp1 was significantly increased [36]. Similar results were observed in the *in vitro* model group with lipid accumulation in the present study. The mitochondria in the FFA group showed significant fragmentation, and the expression of Drp1 increased slightly (although the difference was not significant), whereas the expression of Mfn2 and OPA1 decreased significantly, suggesting that FFA-induced changes in HepG2 cells were affected by the inhibition of mitochondrial fusion and promotion of mitochondrial division. The mitochondrial structure was significantly restored following lactucin treatment, and the relative mRNA expression of *Drp1* was significantly reduced compared to that in the FFA group; however, no significant decrease was detected at the protein level. The expression levels of Mfn2 and OPA1 significantly increased following lactucin treatment. These results suggest that lactucin modulates mitochondrial fusion factors to ameliorate FFA-induced impairment of mitochondrial dynamics in HepG2 cells, rather than by affecting mitochondrial fission factors.

4.5. Regulation of the SIRT1/PGC-1α signalling axis and mitochondrial function by EX527

To further verify the regulation of SIRT1 by lactucin, we used the SIRT1 inhibitor, EX527. EX527 selectively inhibits SIRT1 deacetylase activity. The results revealed that SIRT1 expression was significantly lower in the EX527-treated group compared with that in the lactucin-treated group. PGC-1α, a SIRT1-regulated downstream protein, and the mitochondrial quality control-related proteins including Nrf1, Tfam, Mfn2, and Opa1 were also significantly inhibited to varying degrees in the EX527-treated group. Furthermore, EX527 treatment increased lipid droplet formation, and TG and ROS levels. These changes lead to mitochondrial dysfunction in HepG2 cells by reducing mitochondrial respiratory chain activity, promoting mitochondrial membrane depolarisation, and depleting ATP content. Furthermore, EX527 reversed the lactucin-mediated inhibition of lipid accumulation in a high-fat cell model, increase in mitochondrial biosynthesis, and expression of mitochondrial dynamic-related proteins. Thus, SIRT1 activity plays a key enabling role in the mechanism by which lactucin ameliorates FFA-induced lipid accumulation and mitochondrial damage in HepG2 cells.

5. Conclusions

In summary, the present study revealed that lactucin inhibits FFA-induced impairment of mitochondrial dynamic homeostasis and ameliorates hepatocellular lipid accumulation in an *in vitro* model of MAFLD, potentially via the SIRT1/PGC-1α signalling axis (Fig. 8). To the best of our knowledge, this is the first study to reveal the potential role of lactucin in the prevention of MAFLD through the promotion of mitochondrial function. Thus, this study provides a new research direction for the application of lactucin for MAFLD treatment.

CRediT authorship contribution statement

Yi Lei: Writing – original draft, Validation, Data curation. **Xiao-li Ma:** Writing – original draft, Methodology. **Tong Liu:** Validation. **Meng-jiao Wang:** Validation. **Jin-sen Kang:** Resources. **Jian Yang:** Writing – review & editing, Project administration, Conceptualization. **Na Mi:** Writing – review & editing, Conceptualization.

Data availability statement

The data that support the findings of this study have not been deposited into a publicly available repository, but are available from the corresponding author upon reasonable request.

Ethics and consent declarations

This article does not involve human or animal involvement.

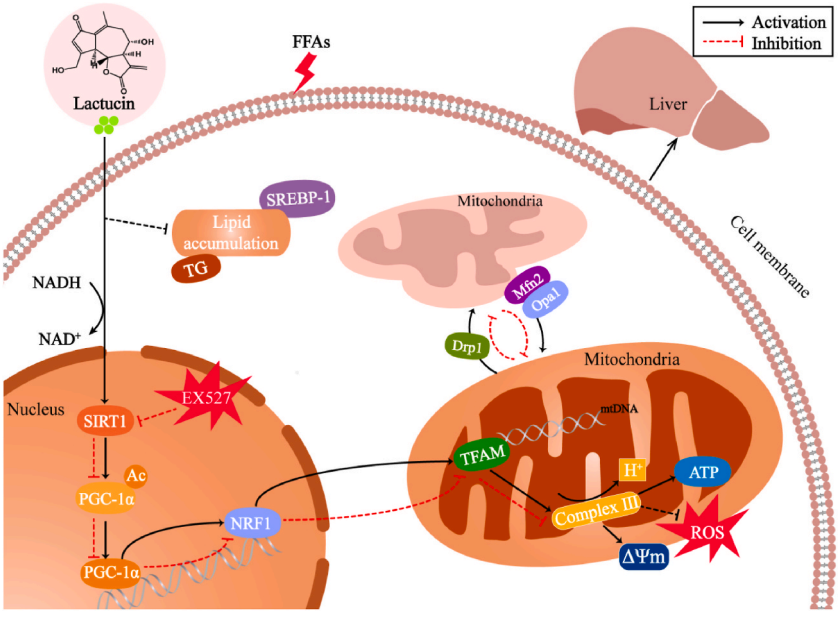

Fig. 8. Lactucin regulates mitochondrial biosynthesis and dynamics through the SIRT1/PGC-1α pathway.

Funding statement

This research was supported by the National Natural Science Foundation of China (Grant No. 82360721),the Natural Science Foundation of Xinjiang Uygur Autonomous Region, China (Grant No. 2021D01C256), and the Xinjiang Uygur Autonomous Region Tianshan Talent Youth Top Talent Project, China (Grant No. 2022TSYCCX0104).

Declaration of competing interest

The authors declare the following financial interests/personal relationships which may be considered as potential competing interests:Jian Yang reports was provided by National Natural Science Foundation of China. Jian Yang reports equipment, drugs, or supplies was provided by the Natural Science Foundation of Xinjiang Uygur Autonomous Region, China. Xiao-li Ma reports equipment, drugs, or supplies was provided by the Xinjiang Uygur Autonomous Region Tianshan Talent Youth Top Talent Project, China. Reports a relationship with that includes:. Has patent pending to. If there are other authors, they declare that they have no known competing financial interests or personal relationships that could have appeared to influence the work reported in this paper.

Abbreviations:	
ATP	Adenosine Triphosphate
CCK-8	Cell Counting Kit-8
CCCP	Carbonyl cyanide 3-chlorophenylhydrazone
DCFH-DA	2,7-Dichlorodihydrofluorescein diacetate
DRP1	Dynamin-related protein 1;
EX527	Selisistat
FFA	Free fatty acid
HepG2	Hepatocellular carcinoma cells
IC50	Half maximal inhibitory concentration
NRF1	Recombinant Nuclear Respiratory Factor 1
OA	Oleic acid
OPA1	Optic atrophy 1
PA	Palmitic acid
PGC-1α	Peroxisome proliferator-activated receptor gamma coactivator 1-alpha
PMSF	Phenylmethylsulfonyl fluoride
ROS	Reactive oxygen spices
SIRT-1	Sirtuin-1
SREBP1	Sterol-regulatory element binding protein 1
TFAM	Mitochondrial transcription factorA
TG	Triglyceride

Appendix A. Supplementary data

Supplementary data to this article can be found online at https://doi.org/10.1016/j.heliyon.2024.e39890.

References

[1] Z.M. Younossi, A.B. Koenig, D. Abdelatif al, Global epidemiology of nonalcoholic fatty liver disease-Meta-analytic assessment of prevalence, incidence, and outcomes, Hepatology 64 (1) (2016) 73–84, https://doi.org/10.1002/hep.28431.
[2] M.H. Le, D.M. Le, T.C. Baez al, Global incidence of non-alcoholic fatty liver disease: a systematic review and meta-analysis of 63 studies and 1,201,807 persons, J. Hepatol. 79 (2) (2023) 287–295, https://doi.org/10.1016/j.jhep.2023.03.040.
[3] E.E. Powell, V.W.S. Wong, M. Rinella, Non-alcoholic fatty liver disease, Lancet 397 (2021) 2212–2224, https://doi.org/10.1016/S0140-6736(20)32511-3.
[4] M. Carmiel-Haggai, A.I. Cederbaum, N. Nieto, A high-fat diet leads to the progression of non-alcoholic fatty liver disease in obese rats, Faseb j 19 (1) (2005) 136–138, https://doi.org/10.1096/fj.04-2291fje.
[5] Q. Chen, T. Wang, J. Li al, Effects of natural products on fructose-induced nonalcoholic fatty liver disease (NAFLD), Nutrients 9 (2) (2017), https://doi.org/10.3390/nu9020096.
[6] G. Paradies, V. Paradies, F.M. Ruggiero al, Oxidative stress, cardiolipin and mitochondrial dysfunction in nonalcoholic fatty liver disease, World J. Gastroenterol. 20 (39) (2014) 14205–14218, https://doi.org/10.3748/wjg.v20.i39.14205.
[7] C.L. Pouille, S. Ouaza, E. Roels, Chicory: understanding the effects and effectors of this functional food, Nutrients 14 (5) (2022), https://doi.org/10.3390/nu14050957.
[8] J.L. Yan, J.S. Kang, B.T. Chen al, Effects of *Cichorium glandulosum* on hyperglycemia, dyslipidemia and intestinal flora in db/db mice, J. Funct.Foods 97 (2022), https://doi.org/10.1016/j.jff.2022.105240.
[9] T. Dang, Chemical Composition and Biological Activity of Chicory, Shihezi University, 2020.
[10] X. Wang, M. Liu, G.H. Cai al, A potential nutraceutical candidate lactucin inhibits adipogenesis through downregulation of JAK2/STAT3 signaling pathway-mediated mitotic clonal expansion, Cells 9 (2) (2020), https://doi.org/10.3390/cells9020331.
[11] Y. Aibaidula, M. Aimaiti, H.W. Tan al, Lactucin & Lactucopicrin ameliorates FFA-induced steatosis in HepG2 cells via modulating lipid metabolism, J. Pharmacol. Sci. 150 (2) (2022) 110–122, https://doi.org/10.1016/j.jphs.2022.07.007.
[12] C. Koliaki, J. Szendroedi, K. Kaul al, Adaptation of hepatic mitochondrial function in humans with non-alcoholic fatty liver is lost in steatohepatitis, Cell Metabol. 21 (5) (2015) 739–746, https://doi.org/10.1016/j.cmet.2015.04.004.

[13] H. Yang, Y. Liu, Y. Wang al, Knockdown of Sirt1 gene in mice results in lipid accumulation in the liver mediated via PGC-1α-induced mitochondrial dysfunction and oxidative stress, Bull. Exp. Biol. Med. 172 (2) (2021) 180–186, https://doi.org/10.1007/s10517-021-05359-1.
[14] H. Si, D. Liu, Dietary antiaging phytochemicals and mechanisms associated with prolonged survival, J. Nutr. Biochem. 25 (6) (2014) 581–591, https://doi.org/10.1016/j.jnutbio.2014.02.001.
[15] T. Ren, L. Zhu, Y. Shen al, Protection of hepatocyte mitochondrial function by blueberry juice and probiotics via SIRT1 regulation in non-alcoholic fatty liver disease, Food Funct. 10 (3) (2019) 1540–1551, https://doi.org/10.1039/c8fo02298d.
[16] M. Ortiz, S.A. Soto-Alarcón, P. Orellana al, Suppression of high-fat diet-induced obesity-associated liver mitochondrial dysfunction by docosahexaenoic acid and hydroxytyrosol co-administration, Dig. Liver Dis. 52 (8) (2020) 895–904, https://doi.org/10.1016/j.dld.2020.04.019.
[17] M.C. Hernández-Rodas, R. Valenzuela, F. Echeverría al, Supplementation with docosahexaenoic acid and extra virgin olive oil prevents liver steatosis induced by a high-fat diet in mice through PPAR-α and Nrf2 upregulation with concomitant SREBP-1c and NF-kB downregulation, Mol. Nutr. Food Res. 61 (12) (2017), https://doi.org/10.1002/mnfr.201700479.
[18] Z. Younossi, Q.M. Anstee, M. Marietti al, Global burden of NAFLD and NASH: trends, predictions, risk factors and prevention, Nat. Rev. Gastroenterol. Hepatol. 15 (1) (2018) 11–20, https://doi.org/10.1038/nrgastro.2017.109.
[19] Q. Chen, Y. Lou, G protein-coupled receptor 39 alleviates mitochondrial dysfunction and hepatocyte lipid accumulation via SIRT1/Nrf2 signaling, J. Bioenerg. Biomembr. 55 (1) (2023) 33–42, https://doi.org/10.1007/s10863-022-09953-4.
[20] G. Kanuri, I. Bergheim, In vitro and in vivo models of non-alcoholic fatty liver disease, Int. J. Mol. Sci. 14 (6) (2013) 11963–11980, https://doi.org/10.3390/ijms140611963.
[21] M.J. Gómez-Lechón, M.T. Donato, A. Martínez-Romero al, A human hepatocellular in vitro model to investigate steatosis, Chem. Biol. Interact. 165 (2) (2007) 106–116, https://doi.org/10.1016/j.cbi.2006.11.004.
[22] H.W. Tan, Y.W. Zhong, Y. Lei, et al., Comparative study on the promotion of FFA-induced lipid metabolism in HepG2 cells by lactucin and lactucopicrin, Chin Food Additives 34 (4) (2023) 60–68.
[23] D. Samardzija Nenadov, B. Tesic, T. Tomanic, Global gene expression analysis reveals a subtle effect of DEHP in human granulosa cell line HGrC1, Reprod. Toxicol. 120 (2023) 108452, https://doi.org/10.1016/j.reprotox.2023.108452.
[24] Y. Wang, S. Hekimi, Mitochondrial dysfunction and longevity in animals: untangling the knot, Science 350 (6265) (2015) 1204–1207, https://doi.org/10.1126/science.aac4357.
[25] A. Carazo, J. León, J. Casado al, Hepatic expression of adiponectin receptors increases with non-alcoholic fatty liver disease progression in morbid obesity in correlation with glutathione peroxidase 1, Obes. Surg. 21 (4) (2011) 492–500, https://doi.org/10.1007/s11695-010-0353-2.
[26] G.H. Lee, C. Peng, S.A. Park al, Citrus peel extract ameliorates high-fat diet-induced NAFLD via activation of AMPK signaling, Nutrients 12 (3) (2020), https://doi.org/10.3390/nu12030673.
[27] W. Gao, B. Xu, Y. Zhang al, Baicalin attenuates oxidative stress in a tissue-engineered liver model of NAFLD by scavenging reactive oxygen species, Nutrients 14 (3) (2022), https://doi.org/10.3390/nu14030541.
[28] A. Khader, W.L. Yang, A. Godwin al, Sirtuin 1 stimulation attenuates ischemic liver injury and enhances mitochondrial recovery and autophagy, Crit. Care Med. 44 (8) (2016) e651–e663, https://doi.org/10.1097/ccm.0000000000001637.
[29] J. Li, M. Liu, H. Yu al, Mangiferin improves hepatic lipid metabolism mainly through its metabolite-norathyriol by modulating SIRT-1/AMPK/SREBP-1c signaling, Front. Pharmacol. 9 (2018) 201, https://doi.org/10.3389/fphar.2018.00201.
[30] M.S. Poornima, G. Sindhu, A. Billu al, Pretreatment of hydroethanolic extract of Dillenia indica L. attenuates oleic acid induced NAFLD in HepG2 cells via modulating SIRT-1/p-LKB-1/AMPK, HMGCR & PPAR-α signaling pathways, J. Ethnopharmacol. 292 (2022) 115237, https://doi.org/10.1016/j.jep.2022.115237.
[31] X.Q. Deng, L.L. Chen, N.X. Li, The expression of SIRT1 in nonalcoholic fatty liver disease induced by high-fat diet in rats, Liver Int. 27 (5) (2007) 708–715, https://doi.org/10.1111/j.1478-3231.2007.01497.x.
[32] Y. Colak, O. Ozturk, E. Senates al, SIRT1 as a potential therapeutic target for treatment of nonalcoholic fatty liver disease, Med Sci Monit 17 (5) (2011) Hy5–9, https://doi.org/10.12659/msm.881749.
[33] C.H. Chiu, M.Y. Chen, J.J. Lieu al, Inhibitory effect of styrylpyrone extract of phellinus linteus on hepatic steatosis in HepG2 cells, Int. J. Mol. Sci. 24 (4) (2023), https://doi.org/10.3390/ijms24043672.
[34] H. Rafiei, K. Omidian, B. Bandy, Dietary polyphenols protect against oleic acid-induced steatosis in an in vitro model of NAFLD by modulating lipid metabolism and improving mitochondrial function, Nutrients 11 (3) (2019), https://doi.org/10.3390/nu11030541.
[35] Y.Y. Zou, X.B. Tang, Z.L. Chen al, Exercise intervention improves mitochondrial quality in non-alcoholic fatty liver disease zebrafish, Front. Endocrinol. 14 (2023) 1162485, https://doi.org/10.3389/fendo.2023.1162485.
[36] J. San, J. Hu, H. Pang al, Taurine protects against the fatty liver hemorrhagic syndrome in laying hens through the regulation of mitochondrial homeostasis, Int. J. Mol. Sci. 24 (12) (2023), https://doi.org/10.3390/ijms241210360.